Proceedings of the 11th ICPMG 2026
11th International Conference on Physical Modelling in Geotechnics
8-12 June 2026, Zurich, Switzerland

Experimental investigation on the load-sharing mechanism of suction bucket foundations under vertical loading in soft clay

Y. Zhang, C. Wu
Southeast University, Nanjing, China, youhuzhang@seu.edu.cn, chuhengwu@seu.edu.cn

B. Bienen
University of Western Australia, Perth, Australia, britta.bienen@uwa.edu.au

ABSTRACT: Suction bucket jacket foundations are an attractive foundation solution for deep water wind development in China as an alternative to piled jackets. A design challenge is long-term tilt due to differential settlement between buckets, driven by prevailing wind directions and soft seabed conditions. Assessing long-term consolidation settlement is complex, with uncertainties in load sharing between the skirt tip, skirt friction and the bucket lid, and load redistribution as soil transitions from undrained to drained behaviour. This study presents centrifuge experiments to investigate the load-sharing mechanisms in suction bucket foundations installed in soft kaolin clay. Two suction bucket models are employed, and three loading conditions are evaluated in this study: idealized constant loading (ICL), time-varying loading (TVL), and constant loading interspersed extreme event (IEE). The experiments examine the initial undrained load distribution and induced excess pore pressure, alongside load redistribution between the skirt and lid as pore pressure dissipates. Results indicate significant load transfer from the lid to the skirt during consolidation and "reverse" transfer in response to cyclic loads, with relevant mechanism being discussed.

1 INTRODUCTION

Suction bucket jackets (SBJ) are an attractive foundation solution for offshore wind development in deep waters in China due to their efficient installation as compared to piled jackets. There are two main features of the geological conditions and marine environment in China's southern eastern coastal regions, where large offshore wind developments are being made:

(1) The seabed surface is extensively covered by recently deposited soft soils. These soils exhibit low undrained shear strength, high water content, and significant consolidation compressibility (Liu et al., 2020).

(2) The dominant wind direction is pronounced, which means during the life time of the turbines, they operates under a relatively fixed incoming wind direction.

Due to the above two features, the buckets of a SBJ are potentially subjected different vertical loads for prolonged periods of time, which can lead to uneven settlement and consequently tilt of the wind turbine structure. For this reason, during the design stage of SBJ in such condtions, it is required to evaluate the long-term consolidation settlements of the bucket foundations and further evaluate the potential tilt caused by different settlments between the buckets. However, to evluate the long-term consolidation settlement of a bucket foundation is not a trival task, which is complicated by several factors:

1) As discussed by Liu et al. (2020) and Zhang et al. (2024), the vertical load sharing between the bucket lid, the internal and external skirt frictions and the skirt tip resistance has a large impact on the distribution of stress increase within the soil plug and the soil beneath the bucket foundation. Therefore, to assess the consolidation settlement of a bucket foundation under vertical load, it is crucial to know how the vertical load is shared between the bucket lid, the skirt frictions and the skirt tip resistance;
2) As the foundation settles under a sustained vertical load, the load sharing changes as the soil transits from undrained response to drained response;
3) As the wind speed varies with time, the magnitudes of vertical load on the bucket foundations also vary with time;
4) The consolidation process is often interrupted by extreme events, such as storms, which can cause short term intensive loading on the buckets. It is uncertain how such short duration but high intensity loading event may influence the long-term consolidation process.

There are relatively few studies reported in the literature on the long-term consolidation settlement of skirted foundations in clay. To support the design of the first SBJ in China (CTG Shapa Phase I SBJ demonstration project), Liu et al. (2020) proposed an analytical settlement calculation model for a bucket foundation under constant vertical load. The model was further refined by Zhang et al. (2024) based on numerical simulation. To verify the theoretical model and to shed light on the more complex loading conditions (time varying vertical load and interuptions of extreme loading events), a series of centrifuge experiments on suction bucket response to long-term vertical loading in soft clay are performed. This paper presents data from the tests. Focus is given to the load sharing mechanism during consolidation, which is essential in calculating the settlement of the suction buckets.

2 EXPERIMENTAL ARRANGEMENT

The experiments were conducted using the 3.6 m diameter beam centrifuge (Randolph et al., 1991) at the National Geotechnical Centrifuge Facility (NGCF) located at The University of Western Australia (UWA). Given the similarity of the experimental setup to previous suction bucket model tests (da Silva Pereira et al., 2024a, 2024b; Stapelfeldt et al., 2021; Low H. E. et al., 2020; Stapelfeldt et al., 2020; Bienen et al., 2018b, 2018a), only a brief description is provided herein.

2.1 Experimental Apparatus

Two suction bucket models were used in the experiments, with the same diameter, D = 80 mm and skirt lengths L of 80 mm and 120 mm, respectively, so that the aspect ratios of the model suction buckets are L/D=1.0 and L/D=1.5, respectively. The models have the same skirt wall thickness t = 0.5 mm. The pictures of these two models are shown in Figure 1, together with the layout of the total pressure transducers (TPTs) and pore pressure transducers (PPTs), which are the same radial distance from the center of the lid invert.

The suction bucket models were deployed using an electromechanical actuator. The installation resistance was measured via an in-line load cell integrated with the actuator's vertical shaft (Figure2). This load cell's output is fed into the actuator's feedback control system, enabling either: (i) maintenance of prescribed self-weight stress during suction-assisted installation, or (ii) generation of the target cyclic loading protocol. Vertical displacements of the lid of the suction bucket were measured with a linear displacement transducer (LDT) that was mounted independently.

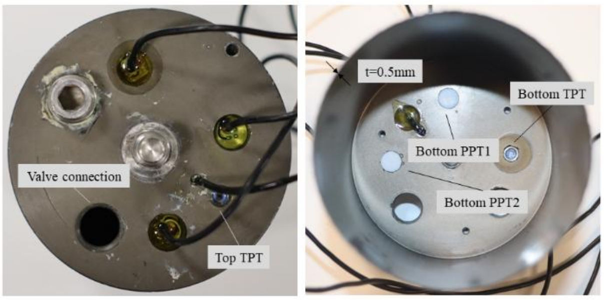

Model with L/D=1.0

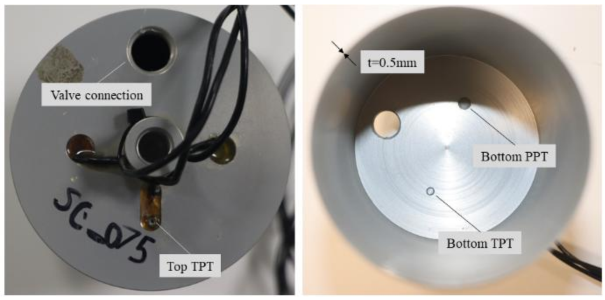

Model with L/D=1.5

Figure 1. Suction bucket models and transducers instrumented

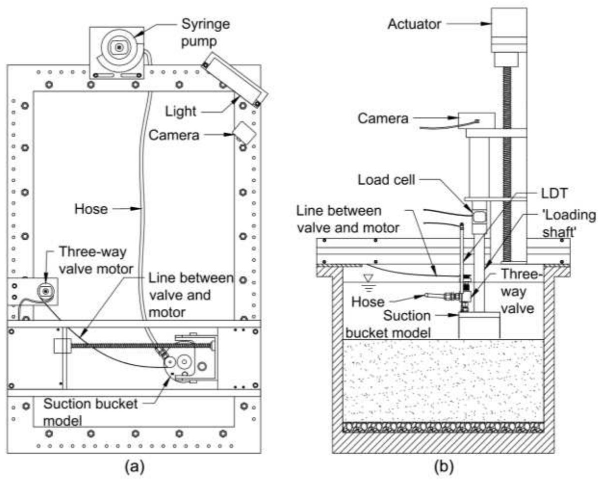

Figure 2. Experimental arrangement: (a) top view;(b) end view (from(Stapelfeldt et al., 2020))

2.2 Sample Preparation and Characterization

One normally consolidated kaolin clay sample was prepared for the experiments. The clay properties of the kaolin used at The University of Western Australia are widely reported, e.g. (Mei et al., 2025; Wang et al., 2023; da Silva Pereira et al., 2024a; Reid et al., 2023) and are summarized in Table 1.

The soil sample was prepared as slurry with a water content of 210% in a large mixer, and the slurry was transferred to the strongbox and consolidated on the centrifuge at an acceleration of 100g for seven days. Two-way drainage for consolidation was provided by a sand layer at the bottom of the strongbox. The internal length and width of the strongbox are 650 mm and 390 mm, respectively. The final height of the soil sample after consolidation is 215 mm.

Sample characterization is carried out using a miniature T-bar penetrometer (Stewart & Randolph, 1994) with a projected penetrating area of $100mm^2$. The tests were carried out at a penetration rate of 1mm/s to ensure undrained conditions. The undrained shear strength (s_u) profile of the clay calculatd using N_{kt}=10.5 is shown in Figure 3. The undrained shear strength exhibits a linear relationship with the effective vertical stress (σ_v'), with a constant s_u/σ_v' ratio of 0.165.

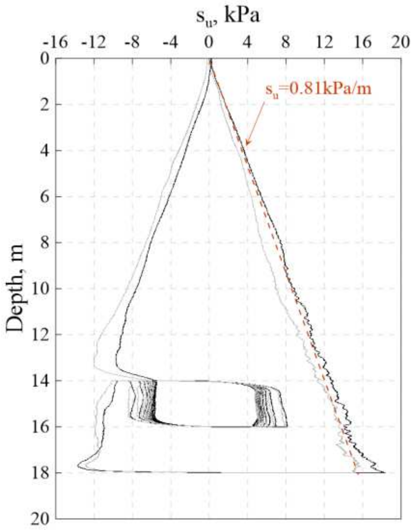

Figure 3. Undrained shear strength profile

Table 1. Properties of UWA Eckalite kaolin clay (da Silva Pereira et al., 2024b; Reid et al., 2023; Wang et al., 2023)

Property	Value
Liquid limit, LL (%)	73.7
Plastic limit, PL(%)	44.4
Specific gravity, G_s	2.6
Plastic index, I_p(%)	29.3
Critical state friction angle, φ_{cs}' (degrees)	23.0 (triaxial)
Gradient of normal compression line, λ	0.435
Swelling index, κ	0.063
Void ratio at p'=1kPa on normally consolidated line (NCL), e_N	3.99

2.3 Experimental Procedures

In the present study, three distinct loading conditions were investigated: (1) ideal constant load (ICL), wherein a constant vertical load was imposed on the suction bucket until full consolidation was achieved, after which the load was either discontinued or incrementally increased; (2) time-varying load (TVL), characterized by stepwise increments/decrements in loading; and (3) interspersed extreme event (IEE), superimposed on a compressive mean load. The ICL is intended to replicate the idealized operational loading of offshore wind turbines under steady wind direction and power output conditions. In contrast, the TVL accounts for more realistic environmental variability, wherein fluctuating wind patterns generate variable loading on the suction buckets. The IEE, meanwhile, addresses infrequent but severe occurrences, such as typhoons. All loading steps are performed after a stabilization period following the suction-aided installation, which allows the residual pore pressure to fully dissipate.

A total of five centrifuge tests were performed across the three loading regimes and two suction bucket geometries. The numeral appended to each loading conditions marks the *L/D* ratio of the corresponding suction bucket. All applied loads were normalized relative to the drained ultimate bearing capacity of skirt friction ($p_{s\_ult\_d}$) of the respective bucket: $p_{s\_ult\_d}$ = 40 kPa for *L/D* = 1.0 and 60 kPa for *L/D* = 1.5, calculated by the method proposed by (Zhang et al., 2024) using the following equation:

$$p_{s\_ult\_d} = 2\int_0^L \pi D \sigma_H' tan\delta dz \qquad (1)$$

where σ_H' is the effective horizontal stress and δ represents the friction angle at the soil-skirt interface. The loading sequences of ICL, TVL and IEE tests are shown in Figure 4 (a), (b) and (c), respectively. The storm load in IEE test is defined as sine wave load with a frequency of 0.5 Hz and 20 cycles. Each storm load lasts for about 4.5 days in prototype.

3 RESULTS

When a vertical load is applied to the suction bucket, a certain proportion of it is initially borne by the lid, as indicated by the total pressure measurements through the TPTs installed on the lid invert. To facilitate discussion, the ratio of the change of load carried by the lid (Δp_{lid}) to the change of total applied load (Δp_{total}), i.e., $\Delta p_{lid}/\Delta p_{total}$ is denoted by r_i in this paper. Upon application of each load increment, the soil responses in an undrained fashion. For interpretation of the test results, the ultimate undrained shaft capacity ($p_{s\_ult\_u}$) is evaluated for both buckets according to the following equation (DNVGL, 2017):

$$p_{s\_ult\_u} = \alpha s_{u(avg)} A_{sur} \quad (2)$$

where α is the interface roughness factor; $s_{u(avg)}$ is the average undrained shear strength along the skirt and A_{sur} is the area of the skirt (including both internal and external shaft areas).

Using an α value of 0.6 (with consideration of set-up after installation), $p_{s\_ult\_u}$ is calculated to be 20 kPa and 36 kPa for L/D=1.0 and L/D=1.5, which are lower than their drained counterparts as calculated by Eq. (1).

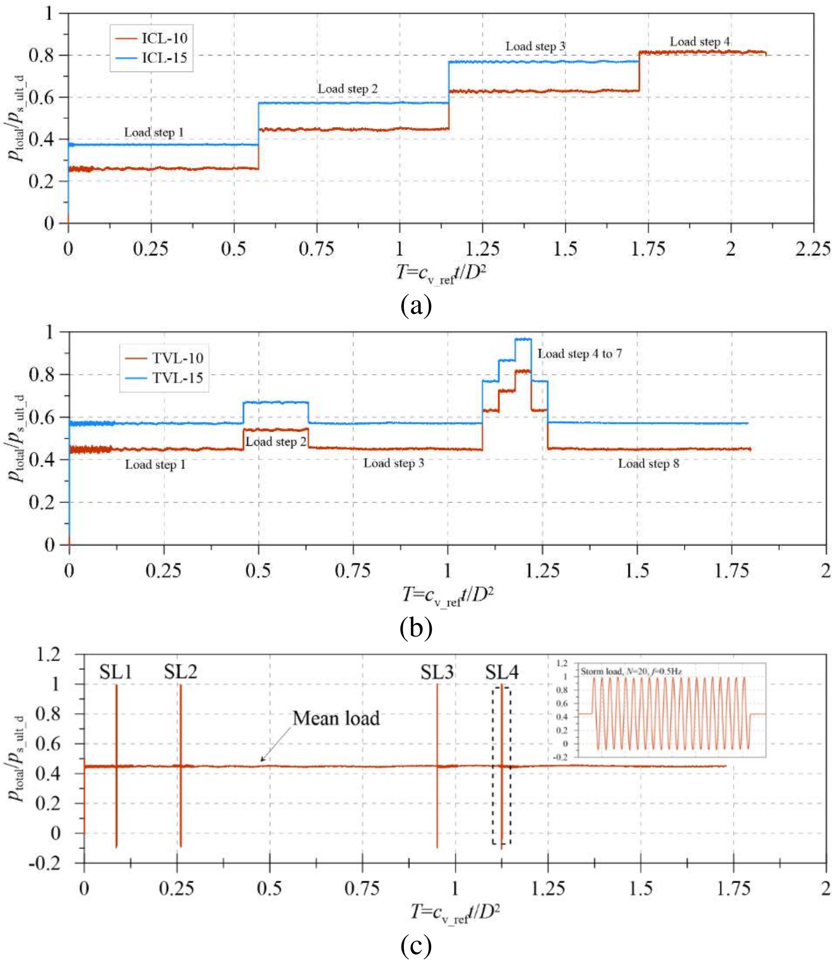

Figure 4. Loading sequences of ICL, TVL and IEE tests

The evolution of initial r_{i_ini} with the ratio of the current load p_l and $p_{s\_ult\_u}$ in ICL and TVL tests is presented in Figure 5. It is clear that the proportion of load carried by the lid increases in an approximately linear fashion with the normalised load level, as illustrated by the results from the ICL tests (Figure 5a). The same trend is followed in the TVL tests in loading steps in which the load on bucket increases (referred as "load rise" hereafter in this paper) except for load Step 4 (Figure 5b). For the load steps in which the load on the bucket reduces in the TVL tests (Steps 3, 7, 8, referred as "load reduction" hereafter in this paper), the load change is mainly responded by the skirt resistance as r_{i_ini} is only 20-40%, which is much lower than the ratio when the load on the bucket rises. As for load Step 4, the r_{i_ini} value is between those for "load rise" and "load reduction". This is because the load change between Step 4 and Step 3 can be divided into two parts: i) load restoration to the load level of Step 2, which follows the same load distribution rule as "load reduction" (i.e., the behaviour for unloading and reloading is the same); ii) load rise from the level of Step 2 to Step 4 which follow the "load rise" distribution rule (i.e., virgin loading).

The accompanying figures (Figure 6 to 10) illustrate the distribution of the total load (p_{total}) between the lid and the skirt (p_{skirt}). Time is normalized using a reference vertical coefficient of consolidation ($c_{v,ref}$ = 1.75 × 10^{-7} m²/s at σ_v' = 20 kPa), as derived from da Silva Pereira et al. (2024a). Red-tinted regions represent the portion carried by the lid, while blue-tinted regions denote the contributions from skirt friction and tip resistance. The change of r_i with the consolidation process of the soil is shown by the green line.

It is clearly demonstrated that the external load variation is distributed to the lid and the skirt at the beginning of each load steps. The load carried by the lid progressively shifts to skirt friction and tip resistance over time, which aligns with the conclusion drawn by Zhang et al. (2024). It can be reasonably inferred that with adequate consolidation time, the lid load can be fully transferred to the skirt, provided sufficient holding capacity of the skirt.

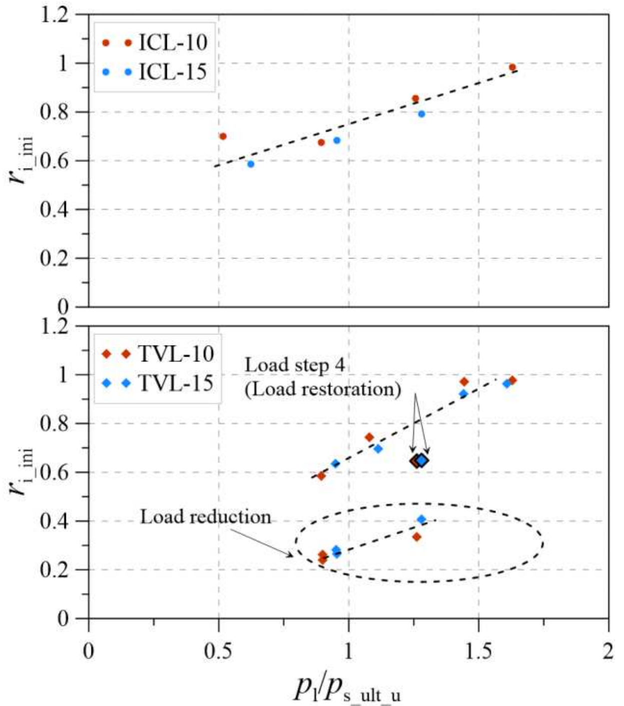

Figure 5. The values of r_{i_ini} *in ICL and TVL tests*

The ICL tests (Figure 6 and 7) composed of several loading steps, the proportion of the load variation carried by the lid at the onset of each load step progressively increases. This trend is likely attributed to the diminishing reserve holding capacity of the skirt. During the load step 1, the skirt possesses ample holding capacity (40kPa for initial loading), allowing it to accommodate a large share of the load variation (around $0.4\Delta p_{total}$). However, as the total load on the bucket increase in subsequent load steps, the residual capacity of the skirt diminishes, prompting a greater reliance on the lid. This is evidenced by the relatively lower initial values of r_i in models with an aspect ratio (L/D) of 1.5 compared to those with L/D = 1.0. For a given diameter, longer skirt provides greater skirt capacity, leading to less load initially borne by the bucket lid. This observation is consistent with the findings from numerical simulations reported by Zhang et al. (2024).

In TVL tests (Figure 8 and 9), the load sequences become not purely ascending and contain load reduction steps. Load reduction results in reduction in excess pore pressure at the lid invert, potentially generating negative pore pressures if the initial excess pore pressure is minimal (Step 8 in TVL-10 and Steps 3, 8 in TVL-15). Following this drop, the excess pore pressure — whether positive or negative — gradually dissipates with time.

In the load restoration step subsequent to load reduction (Step 4 in TVL tests), the proportion of the load variation carried by the lid is notably constrained relative to purely ascending sequences. This phenomenon likely arises from the contact stiffness reduction between the lid invert and the underlying soil due to soil consolidation. Moreover, negative pore pressures developed during load reduction potentially induce partly detachment on the interface, further reducing the contact stiffness. Consequently, during load restoration step, the holding capacity of the skirt and tip mobilizes preferentially, thereby restricting the lid's contribution to the load variation.

In the IEE test illustrated in Figure 10, the load initially carried by the skirt shifts toward the lid following storm loads. The change in excess pore pressure mainly originates from the difference between the cut-in and cut-out load levels at the start and the end of storm loads (p_{oi}), as illustrated in Figure 11. The four sub-figures in Figure 10 shows the zoom-in view of the 4 storm loads. They are SL 1 to 4 from (a) to (d) and the labels on the horizontal axis are omitted to accommodate the layout.

During the first quarter-cycle (load raise) of the first storm load cycle, the load variation is distributed between the lid and the skirt following the proportion ($r_i \approx 75\%$) mentioned above. Subsequently, in the second and third quarter-cycles (load reduction), the load variation is distributed according to the unloading proportion ($r_i \approx 40\%$). In the fourth quarter-cycle (load restoration), it follows the reloading proportion ($r_i \approx 40\%$). This pattern (load reduction and restoration) continues in subsequent cycles and the value of p_{oi} gradually converge. It should be noted that, due to the sharp load decrease during the unloading phases of storm loads, the reloading proportion is lower than that observed in the TVL tests ($r_i \approx 60\%$).

In summary, the essence of the "reverse" load transfer following storm loading lies in the different initial distribution proportions of the lid for load variation at different loading phases (load raise, load reduction, load restoration).

Figure 12 depicts the proportion of load carried by the lid during storm loading in test IEE-10, where p_{lid_pv} represents the peak-to-valley distance in the p_{lid} curve, and p_{total_pv} denotes the corresponding distance in the total force (p_{total}) curve. Within each storm load, the ratio of these parameters remains nearly constant. As consolidation progresses, this proportion exhibits a slight decline, signifying an increasing reliance on the skirt holding capacity.

Figure 13 illustrates the excess pore pressure accumulation across the storm loads in test IEE-10 over the full consolidation period. In the early consolidation phase (SL 1 and 2), approximately half of the pore pressure fluctuation ultimately contributes to net accumulation; this proportion diminishes by 6–7% in the later stages (SL 3 and 4).

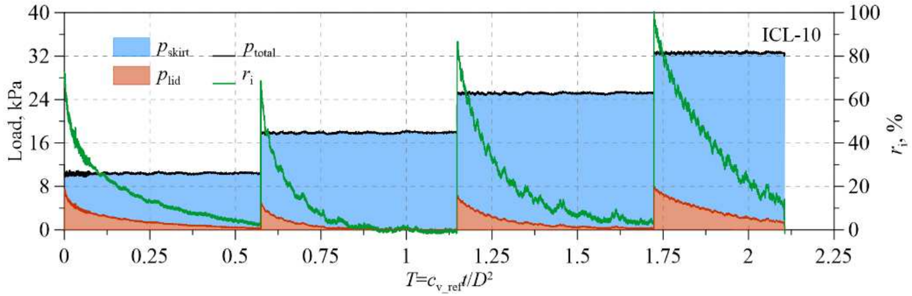

Figure 6. The load transfer during test ICL-10

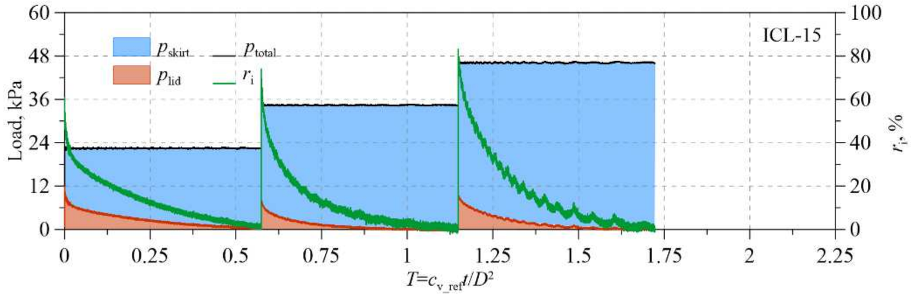

Figure 7. The load transfer during test ICL-15

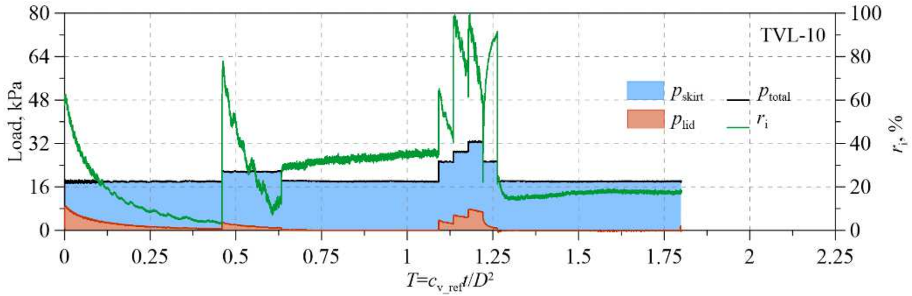

Figure 8. The load transfer during test TVL-10

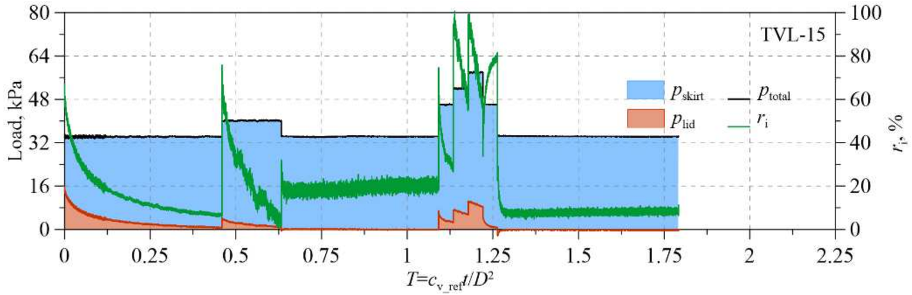

Figure 9. The load transfer during test TVL-15

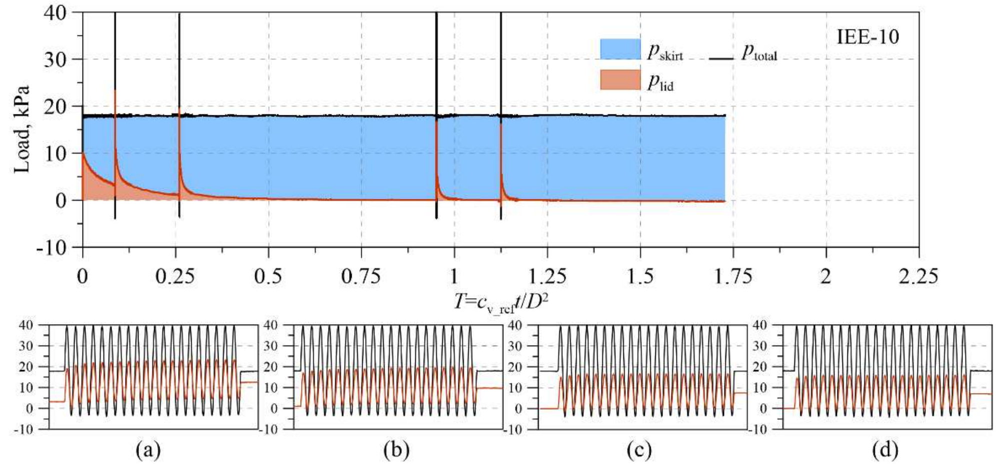

Figure 10. The load transfer during test IEE-10

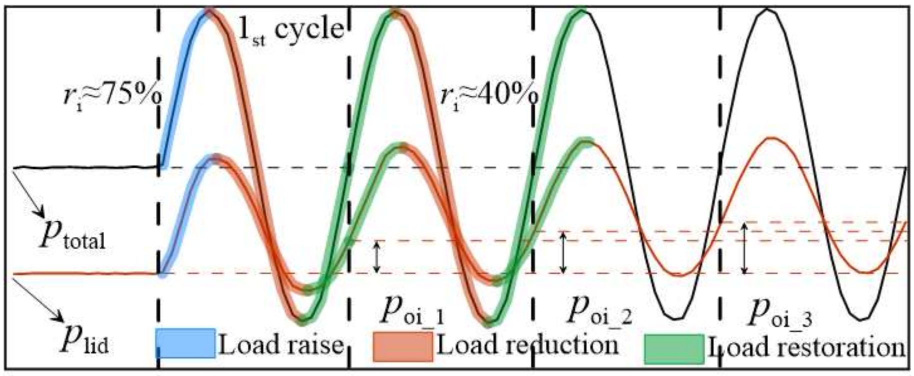

Figure 11. Excess pore pressure accumulation process in storm loads

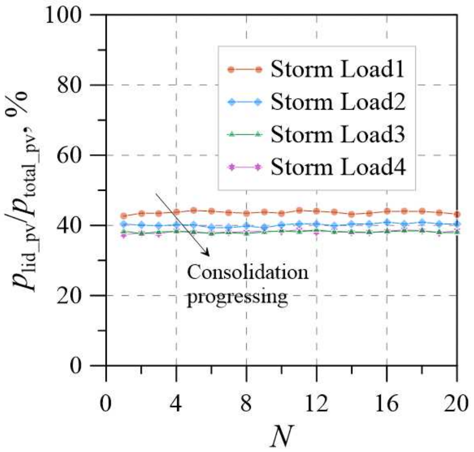

Figure 12. Proportion of load carried by the lid during storm loads in test IEE-10

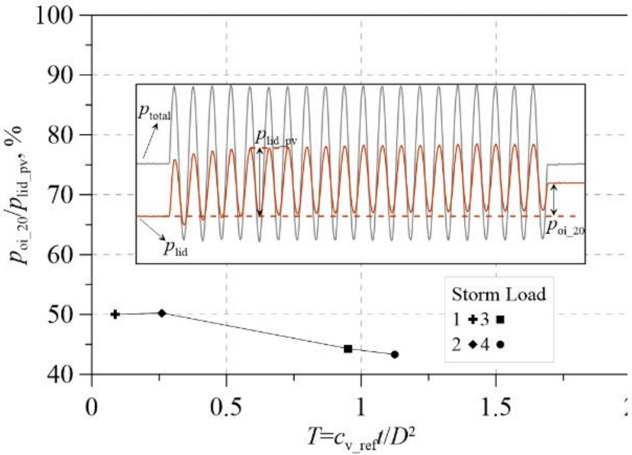

Figure 13. Final excess pore pressure accumulation of each storm load in test IEE-10

4 CONCLUSIONS

This study investigates the response of suction bucket foundations under vertical loading in soft clay, utilizing centrifuge test data to examine load-sharing mechanisms during consolidation.

The vertical load is shared among the lid and the skirt of the suction bucket, with the initial load sharing governed by the soil strength profile, the bucket's aspect ratio (*L/D*), load magnitude, and load history (load raise, load reduction or load restoration).

During consolidation, the load carried by the lid progressively transfers to the skirt, and the lid ultimately carries no load provided sufficient capacity of the skirt. During load reduction, excess pore pressure at the lid invert dissipates rapidly, potentially yielding negative pressures that markedly alter load distribution in subsequent load restoration step.

For interspersed cyclic loading amid mean-load consolidation, the cyclic excursions prompt a reversal in load transfer, which results from the different distribution proportion of load variation on the lid for different load steps (load raise, load reduction, load restoration). Cyclic loading induces excess pore pressure fluctuation at the lid invert with an amplitude of approximately 40% of the cyclic load amplitude, which diminishes slightly in later consolidation stages. 40% to 50% of the excess pore pressure amplitude is transferred to the lid from the skirt at the end of each storm load with the proportion decreasing over time.

REFERENCES

Bienen, B., Klinkvort, R. T., O'Loughlin, C. D., Zhu, F., & Byrne, B. W. (2018a). Suction caissons in dense sand, part I: Installation, limiting capacity and drainage. *Géotechnique*, *68*(11), 937–952. https://doi.org/10.1680/jgeot.16.P.281

Bienen, B., Klinkvort, R. T., O'Loughlin, C. D., Zhu, F., & Byrne, B. W. (2018b). Suction caissons in dense sand, part II: Vertical cyclic loading into tension. *Géotechnique*, 68(11), 953–967. https://doi.org/10.1680/jgeot.16.P.282

da Silva Pereira, F., Bienen, B., & O'Loughlin, C. D. (2024a). Investigation of the Load-Sharing Mechanisms of Suction Buckets during Vertical Cyclic Loading in Layered Soils. *Journal of Geotechnical and Geoenvironmental Engineering*, *150*(10), 04024094. https://doi.org/10.1061/JGGEFK.GTENG-12262

da Silva Pereira, F., Bienen, B., & O'Loughlin, C. D. (2024b). Mind the gap – an experimental study on the need for grouting suction buckets in sand under vertical cyclic loading. *Géotechnique*, *74*(12), 1487–1502. https://doi.org/10.1680/jgeot.22.00174

DNVGL. (2017). *Geotechnical design and installation of suction anchors in clay* (Recommended Practice No. DNVGL-RP-E303; Version April 2017).

Liu, B., Zhang, Y., Ma, Z., Andersen, K. H., Jostad, H. P., Liu, D., & Pei, A. (2020). Design considerations of suction caisson foundations for offshore wind turbines in Southern China. *Applied Ocean Research*, *104*, 102358. https://doi.org/10.1016/j.apor.2020.102358

Low H. E., Zhu, F., Mohr, H., Erbrich, C., Watson, P., Bransby, F., O'Loughlin, C., Randolph, M., Mekkawy, M., & Travasarou, T. (2020). *Cyclic Loading of Offshore Wind Turbine Suction Bucket Foundations in Sand: The Importance of Loading Frequency*. In Proc., 4th Int. Symp. on Frontiers in Offshore Geotechnics., Austin, Texas. https://doi.org/10.1115/OMAE2021%20-62260.

Mei, S., Tian, Y., Cassidy, M. J., & O'Loughlin, C. (2025). Experimental Investigation of Rate Effects on the Uplift Response of Surface and Skirted Circular Shallow Foundations. *Journal of Geotechnical and Geoenvironmental Engineering*, *151*(1), 04024149. https://doi.org/10.1061/JGGEFK.GTENG-12519

Randolph M.F., R. J. Jewell, K. J. L. Stone, & T. A. Brown. (1991). *Establishing a new centrifuge facility* (Hon-Yim Ko & Francis G. Mclean, Eds.).

Reid, D., Fanni, R., & Fourie, A. (2023). A SHANSEP approach to quantifying the behaviour of clayey soils on a constant shear drained stress path. *Canadian Geotechnical Journal*, *61*(8), 1517–1540. https://doi.org/10.1139/cgj-2022-0473

Stapelfeldt, M., Bienen, B., & Grabe, J. (2020). The influence of the drainage regime on the installation and the response to vertical cyclic loading of suction caissons in dense sand. *Ocean Engineering*, *215*, 107105. https://doi.org/10.1016/j.oceaneng.2020.107105

Stapelfeldt, M., Bienen, B., & Grabe, J. (2021). Influence of Low-Permeability Layers on the Installation and the Response to Vertical Cyclic Loading of Suction Caissons. *Journal of Geotechnical and Geoenvironmental Engineering*, *147*(8), 04021076. https://doi.org/10.1061/(ASCE)GT.1943-5606.0002522

Stewart, D. P., & Randolph, M. F. (1994). T-Bar Penetration Testing in Soft Clay. *J. Geotech. Geoenviron. Engng*, *120*(12), 2230–2235. https://doi.org/10.1061/(ASCE)0733-9410(1994)120:12(2230)

Wang, C., O'Loughlin, C. D., Bransby, M., Watson, P., & Zhou, Z. (2023). Consolidation-induced improvements in plate anchor capacity. *Canadian Geotechnical Journal*, *60*(8), 1264–1275. https://doi.org/10.1139/cgj-2022-0382

Zhang, Y., Zhao, S., Zhou, H., Andersen, K. H., & Liu, B. (2024). Long-term settlement of suction bucket foundations supporting offshore wind turbines in clay. *Applied Ocean Research*, *145*, 103922. https://doi.org/10.1016/j.apor.2024.103922